Int. J. Pure Appl. Sci. Technol., 31(2) (2015), pp. 26-39

International Journal of Pure and Applied Sciences and Technology

ISSN 2229 - 6107

Available online atwww.ijopaasat.in

Research Paper

Photo Thermal Response Study of a White Biased Bifacial Silicon Solar Cell under Magnetic Field

Mame Faty Mbaye Fall[1], Moussa Ibra Ngom[1], Marcel Sitor Diouf Gokhan Sahin[1], AmarThiam[1] and GrégoireSissoko[1,*]

[1] University of Cheikh Anta Diop, Faculty of Sciences and Techniques, Physics Department, Dakar, Senegal

* Corresponding author, e-mail: (gsissoko@yahoo.com)

(Received: 2-9-15; Accepted: 17-12-15)

Abstract: *In this paper, we present a photo thermal response study, for a back side illuminated bifacial silicon solar cell under magnetic field by thermal dynamic impedance representations through Nyquist and Bode diagrams.*

Keywords: Photothermal, Impedance, Magnetic field.

Introduction

The efficiency of a solar cell depends among others on its intrinsic parameters. Various characterization techniques have been implemented both in static frequency regime (Barro et al., 2001; Lemrabott et al., 2008) and in dynamic transient regime (Dieng et al., 2007; Barro et al., 2003).

In this present article, we initially will make a short description of the photo voltaic cell bifacial and then we will see the evolution of the density of minority carriers according to the depth and of the intensity of the magnetic field. We then will study the thermal behavior of the photo voltaic cell. We also will study the influence of the pulsation on these parameters. Through the operating performances of Nyquist and Bode plots for the thermal impedance, we established an equivalent electrical circuit of the photocell.

Theory

Photovoltaic Response (Minority Carriers' Density in Excess)

We consider solar silicon with a Back Surface Field (B.S.F) for the structure n+-p-p+ (Le Quang Nam et al, 1992).

Given that the contribution of the base to the photo current is larger than that of the emitter (Barro et al 2001, Lemrabott et al., 2008), the univariate analysis will only be developed in the base region. In addition, we consider the hypothesis of Quasi-Neutral Base (Q.N.B) neglecting the crystal field within the solar cell.

In Fig.1, we present a schematic sketch of a multi crystalline silicon solar cell with a Back Field (BSF) typically n+-p-p+ in a magnetic field.

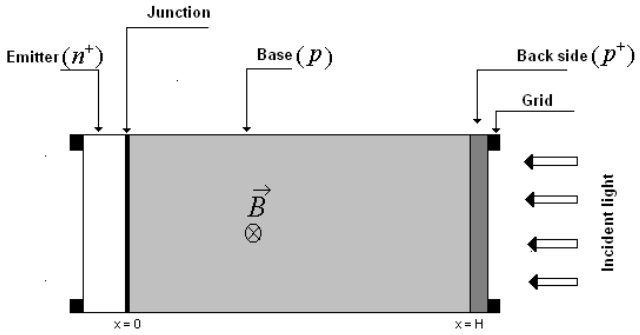

Fig. 1: An n + -p-p + type of a silicon solar cell structure under applied magnetic field (lit by its back face)

When the photo voltaic cell receives a solar radiation, the transformation is done in three stages:

- ✓ Absorption of the photons by material.
- ✓ Creation of pairs electron-positron pair which will be separated by an intense electric field on the level from the zone of space charge.
- ✓ Collection of the particles in an external circuit.

The solar cell is subjected to a constant multi spectra illumination from a source of a modulated frequency and under magnetic field effect and the phenomena of generation, diffusion and recombination of photo gendered carriers in the base are considered. These phenomena are governed by the continuity equation:

$$D(\omega,B)\frac{\partial^2\delta(x,t,\omega,B)}{\partial x^2}-\frac{\delta(x,t,\omega,B)}{\tau}+G(x,t)=\frac{\partial\delta(x,t,\omega,B)}{\partial t} \quad (1)$$

$\delta(x,t)$ The density of the minority carriers in the base which can be written in the form:

$$\delta(x,t)=\delta(x).e^{i.\omega.t} \quad (2)$$

$g(x,t)$ The optical rate of generation given by the expression:

$$G(x,t)=g(x).e^{i.\omega.t} \quad (3)$$

$\delta(x)$ and $g(x)$ represent respectively the spatial components of the minority carrier density and the rate of generation.

And the term $e^{i\omega t}$ represents the time component for the minority carrier density and the rate of optical generation.

Comparing the above equations for which incident optical beam and the density of photo generated carriers, the Eq. (1) is simplified and becomes as follows:

$$\frac{\partial^2 \delta(x)}{\partial x^2} - \frac{\delta(x)}{L(\omega, B)^2} + \frac{g(x)}{D(\omega, B)} = 0 \tag{4}$$

The coefficient *D* which describes the diffusive character of the minority carriers in material, is function of the frequency of modulation and the intensity of the magnetic field and is given by the expression: (Neugroschel *et al*., 1978)

$$D(\omega, B) = D_0 . \frac{\left[1 + \tau^2\left(\omega_c(B)^2 + \omega^2\right) + i\omega\tau\left[\tau^2\left(\omega_c(B)^2 - \omega^2\right) - 1\right]\right]}{4\tau^2\omega^2 + \left[1 + \tau^2\left(\omega_c(B)^2 - \omega^2\right)\right]^2} \tag{5}$$

And $$\frac{1}{L(\omega)^2} = \frac{1}{Ln^2} \times (i\omega\tau + 1) \tag{6}$$

Where $L(\omega, B)$ is the complex scattering length.

The spatial component g(x) is a rate of optical generation of electron-hole pairs for a multi spectral illumination from a constant modulated frequency and as it reflects the entire spectrum of useful radiation incident on the solar cell, it is thus given by the following expression:

$$g_\gamma(x) = \sum_{\lambda_0}^{\lambda_g} \alpha(\lambda)\phi(\lambda)(1 - R(\lambda))\left(\xi e^{-\alpha(\lambda)x} + \chi e^{-\alpha(\lambda)(H-x)}\right) \tag{7}$$

Where $\alpha(\lambda)$ and $R(\lambda)$ represent respectively the absorption coefficient and the reflection coefficient of the material for a given wavelength λ;

$\phi(\lambda)$: Is the flux of incident photons.

λ_g : Wavelength of cut of the semiconductor estimated at 1, 12 µm

λ_0 : The minimal wavelength of the source luminous is equal to 0, 3 µm;

H : The solar cell base thickness.

τ : Is the average lifetime of the minority carriers of load.

The density of minority carriers of load in excess (Electrons) is given by the expression:

$$\delta(x) = A(\omega, B)\cosh\left(\frac{x}{L(\omega, B)}\right) + B(\omega, B)\sinh\left(\frac{x}{L(\omega, B)}\right) + \sum_{\lambda_0}^{\lambda_g} k(\omega, \lambda, B)\left(e^{-\alpha(\lambda)(H-x)}\right) \tag{8}$$

With

$$k(\omega, \lambda, B) = \frac{\alpha(\lambda)\phi(\lambda)(1 - R(\lambda))\, L(\omega, B)^2}{D(\omega, B)^2 (1 - L(\omega, B)^2\, \alpha(\lambda)^2)} \tag{9}$$

Using the boundary conditions (Dieng et al., 2007) presented in Eq. (10) and (11), the coefficients $A(\omega, B)$ and $B(\omega, B)$ are determined.

At the emitter-base junction (x = 0) of the solar cell:

$$\frac{\partial \delta(x)}{\partial x}\Big|_{x=0} = Sf \ \frac{\delta\ (0)}{D(\omega)} \tag{10}$$

At the rear side of the cell base (x = H):

$$\frac{\partial \delta\ (x)}{\partial x}\Big|_{x=H} = -Sb \ \frac{\delta\ (H)}{D(\omega)} \tag{11}$$

Sf and *Sb* are respectively the recombination velocity at the junction and at the rear surface of the base.

There combination velocity *Sf* is imposed by a varying impedance of an external load and by the interface states at the junction:

$$Sf = Sf0 + Sfm \tag{12}$$

Indeed, *Sf* is the sum of two contributions:

*Sf*0 is the intrinsic recombination velocity (depending only on the intrinsic parameters of the solar cell and is induced by the shunt resistor), *Sfm* reflects the leakage current induced by the external load and for the operating point of the solar cell (Diallo et al., 2008; Dème et al., 2009).

Photo-thermal Response (Excess Temperature across the Solar Cell)

When a solar cell is subjected to a multispectral optical excitation from a constant modulated frequency and under magnetic field, the minority charge carriers (electrons) are generated in the base. The movement of such carriers (diffusion and migration) in the solar cell generates a heat flux and an excessive temperature different from the equilibrium temperature of the material. (Dème et al, 2009).

For a small temperature change compared to the initial temperature. To, the heat flux in the solar cell can be described by this equation:

$$a \cdot \frac{\partial^2 \Delta T(x,t,B)}{\partial x^2} + \frac{G_H(x,t,B)}{\rho \cdot c} = \frac{\partial \Delta T(x,t,B)}{\partial t} \tag{13}$$

a is the thermal diffusivity of material, ρ the density and C its specific heat.

The terms ΔT(x, t, B) and G_H(x, t, B) which represent the change in temperature from the initial temperature T_o and the rate of heat generation with time written:

$$\Delta T(x,t,B) = \Delta T(x,B) \cdot e^{i \cdot \omega t} \tag{14}$$

$$G_H(x,t,B) = G_H(x,B)^{\pm} e^{i \cdot \omega t} \tag{15}$$

ΔT(x, B) and G_H(x, B) are the spatial components of the temperature and rate of heat generation.

The term $e^{j\cdot\omega t}$ represents the time component of the temperature and rate of heat generation. This time component has the same pulse $\omega = 2\cdot\pi\cdot f$ as the incident optical beam at each time t.

Equation (13) can be rewritten:

$$\frac{\partial^2 \Delta T(x,B)}{\partial x^2} - \sigma(\omega)^2 \Delta T(x,B) + \frac{G_H(x,B)}{k} = 0 \tag{16}$$

With

K = a.ρ.c is the thermal conductivity of the material $\sigma(\omega) = \left(\frac{i\cdot\omega}{a}\right)^{1/2}$ is the complex thermal diffusion coefficient of the material.

The spatial component $G_H(x,B)$ of the rate of heat generation is given by the equation:

$$G_H(x,B) = \sum_{\lambda_0}^{\lambda_g} \alpha(\lambda).\phi(\lambda).[1-R(\lambda)].\Delta E(\lambda).e^{-\alpha(\lambda)x} + \frac{E_g.\delta(x)}{\tau} \tag{17}$$

With E_g is the energy gap of the semiconductor material $\Delta E = h.\upsilon - Eg$ is the energy thermalization resulting from the relaxation of optically excited carriers was due to absorption of photons of energy greater than the energy gap Eg.

The heat Equation (13) can be expressed as:

$$\begin{aligned}&\frac{d^2\Delta T(x,B)}{dx^2} - \sigma(\omega,B)^2.\Delta T(x,B) = \frac{E_g}{k\tau}\left\{A_1(\omega,B).ch\left(\frac{x}{L_\omega}\right) + A_2(\omega,B).sh\left(\frac{x}{L_\omega}\right)\right\}\\ &-\sum_{\lambda_0}^{\lambda g}\frac{\alpha(\lambda).\phi(\lambda).[1-R(\lambda)]}{k}\left\{\Delta E + \frac{E_g.L(\omega,B)^2}{D(\omega,B).\tau.(1-\alpha^2.L^2\omega)}\right\}.e^{-\alpha(\lambda).x}\end{aligned} \tag{18}$$

The excess temperature of the movement of minority carriers in the material, solution of the above equation is of the form:

$$\begin{aligned}&\Delta T(x,\omega,B,m) = C_1(\omega,B,m).ch(\sigma.x) + C_2(\omega,B,m).sh(\sigma.x)\\ &+\frac{E_g}{k.\tau.(\sigma(\omega)^2 - L(\omega,B)^2)}\left\{A_1(\omega,B,m).ch\left(\frac{x}{L(\omega,B)}\right) + A_2(\omega,B,m).sh\left(\frac{x}{L(\omega,B}\right)\right\}\\ &+\sum_{\lambda_0}^{\lambda_g}\frac{\alpha(\lambda).\phi(\lambda).[1-R(\lambda)]}{k.[\sigma(\omega)^2 - \alpha(\lambda)^2]}\left\{\Delta E + \frac{E_g.L(\omega,B)^2}{D(\omega,B).\tau.[1-\alpha(\lambda)^2.L(\omega,B)^2]}\right\}.e^{-\alpha(\lambda).x}\end{aligned} \tag{19}$$

The coefficients C1(ω, B, m) and C2(ω, B, m) are determined by the following boundary conditions: At the emitter-base junction (x = 0)

$$\frac{\partial \Delta T\ (x,\omega;B)}{\partial x}\Big|_{x=0} = Sf\ \frac{Eg\,\delta(x=0,\omega;B)}{k} \tag{20}$$

At the rear of the base (x = H):

$$\frac{\partial \Delta T(x,\omega,B)}{\partial x}\Big|_{x=H} = -Sb\,\frac{Eg\,\delta\ (\omega,x=H,B)}{k'} \tag{21}$$

Results

Photovoltaic Response (Profile of the Minority Carrier Density)

Figure 2 show the profile curves of module density of charge carriers in the base of the solar cell.

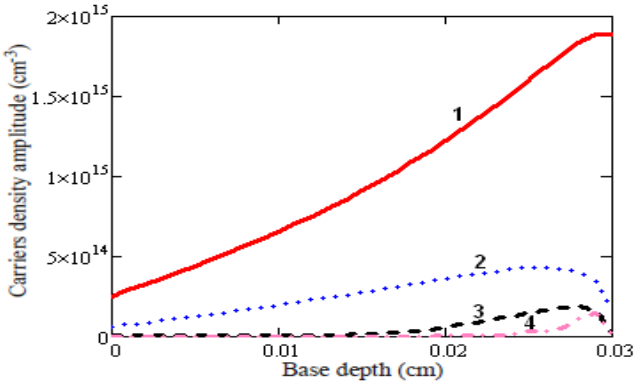

Fig. 2: Minority carrier density versus the base depth for different values of the magnetic field

(H=0.03 μ m; D=26cm^2/s)

1) B=0 (T), ω=0 rad/s;
2) B=10^{-6} (T), ω=1.7782.10^5 rad/s;
3) B=10^{-5} (T), ω=1.7769.10^6 rad/s;
4) B=10^{-4} (T), ω=1.7611.10^7 rad/s

The curves show that the density of the minority carriers believes with depth x in the base to reach their maximum close to the back face since they are generated on this level. After this threshold; the density decreases. (I. Ly et al, 2011, O. Brahim et al, 2011) One notes also a reduction in the density of the minority carriers with the magnetic field. And here contrary to illumination by the front face the maximum ones are located opposite back with a displacement towards the junction base-collector when the intensity of the magnetic field and the frequency of modulation increase. The magnetic field then causes storage of the carriers opposite back (N. Thiam et al, 2013).

Photothermal Response (Profile of the Temperature Variation)

Figure 3 and 4 show the profile curves of the temperature variation in the base of the solar cell

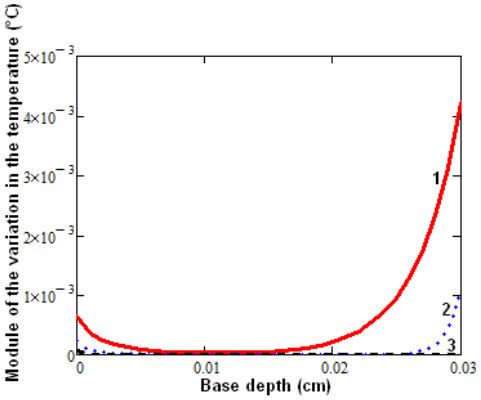

Fig. 3: Module of the temperature variation according to depth x in the base for different values from the magnetic field

1) $B=10^{-6}$(T), $\omega=1.7782.10^{5}$ rad/s;
2) $B=10^{-5}$ (T), $\omega=1.7769.10^{6}$ rad/s;
3) $B=10^{-4}$ (T), $\omega=1.7611.10^{7}$ rad/s

The module of the variation in the temperature decreases close to the junction before cancelling itself in depth. However, one notes an increase in this module on the level of the back zone because the carriers are generated on this level and thus there is more shock involving a heat emission. The amplitude of the module of the variation in the temperature decreases with the presence of the magnetic field.

Profile of the Temperature Variation According to the Junction Recombination Velocity

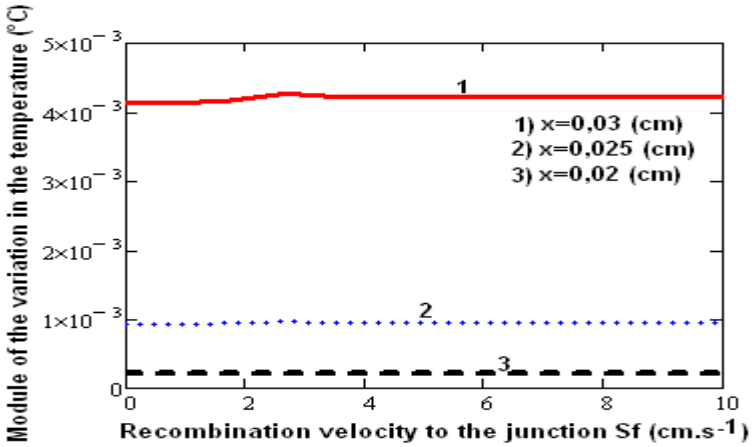

Fig. 4: Module of the variation in the temperature according to the junction recombination velocity for various values depth for an illumination by the back face. (D=26 cm^2/s H=0.03 µm, a=1cm^2/s, k'=1, 54 W/cm. °C)

The curves of the figure 4 show that the variation in the temperature increases with the junction recombination velocity. This is due to the fact that the junction recombination velocity thus translates a movement of the minority carriers into the junction. More the carriers move, more the temperature increases. Moreover the temperature variation believes with the depth in the base. Indeed with this mode of illumination, the charge carriers are generated very close to the face postpones and much of them recombine before thus reaching the base. The storage of the excess minority carriers close to this back face explains this increase in temperature to its vicinity. (Andreas Mandelis, 1989).

Profile of the Density Flux

The expression of the density flux of heat is given by the following relation (22):

$$\phi(x,\omega,B,m) = -k\frac{\partial \Delta T(x,\omega,B,m)}{\partial x} \quad (22)$$

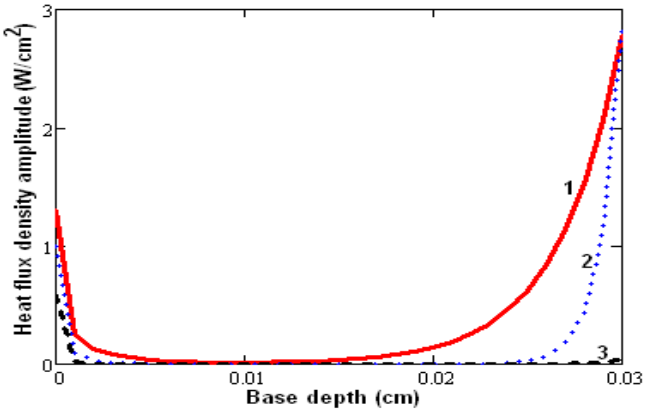

Fig. 5: Module of the density of heat flux as a function of depth for different values of the magnetic field (D=26cm^2/s, H=0.03µm, a=1cm^2/s, k=1,54W/cm. °C)

1) B=10^{-6} (T), ω=1,7782.10^5 rad/s;
2) B=10^{-5} (T), ω=1,7769.10^6 rad/s;
3) B=10^{-4} (T), ω=1,7611.10^7 rad/s

The density flux of heat presents the same evolution as the temperature variation. Close to the junction, it decreases according to the depth then is cancelled; then it increases significantly close to the back face. The amplitude e of the density flux of heat decreases when the intensity of the magnetic field increases.

Profile of the Thermal Impedance

The expression of the thermal impedance (Ould Brahim et al., 2011) is given by the following relation (23)

$$Z(x,\omega,B,m)=\frac{\Delta T(x,\omega,B,m)}{\phi(x,\omega,B,m)} \quad (23)$$

Through the Bode diagram of the impedance, the evolution of module of the impedance as a function of logarithm of the pulsation is presented in Fig. 6 and 8.

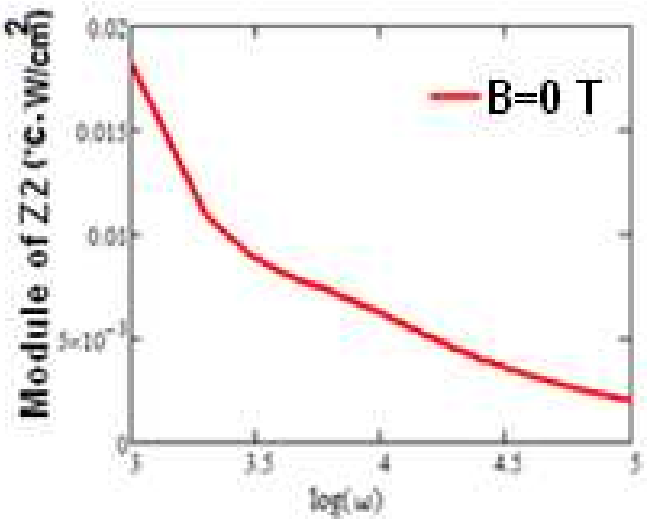

Fig. 6: Module of the thermal impedance according to the logarithm of the pulsation for a null magnetic field

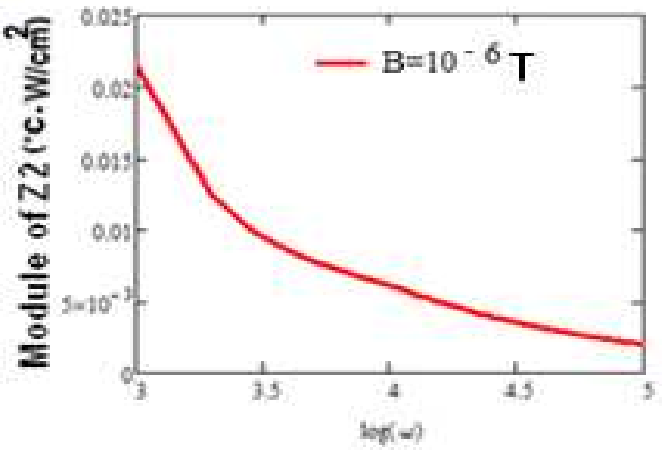

Fig. 7: Module of the thermal impedance according to the logarithm of the pulsation in the presence of the magnetic field

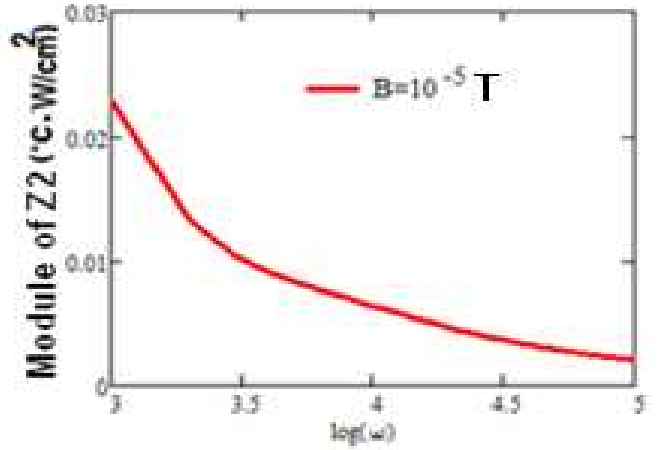

Fig. 8: Module of the thermal impedance according to the logarithm of the pulsation in the presence of the magnetic field

The curves of figures 7, 8 and 9 shows that the module of the thermal impedance is a decreasing function of the pulsation. The increase in the pulsation involves a reduction in the density of the minority carriers and consequently a reduction in the temperature. In this field, the capacitive effects appear there.

Moreover, the application of the magnetic field increases the value of the module of the impedance. (I. Diagne et al, 2008; N. Thiam et al, 2013, M.F. Mbaye et al, 2013).

Bode Diagram of the Impedance for an Illumination by the Back Face: Phase of Zph

$$\varphi(x,\omega,B,m) = \arg(Zph(x,\omega,B,m) \quad (24)$$

$\varphi(x,\omega,B,m)$ Is the phase of the thermal Impedance.

Through the Bode diagram of the impedance, the evolution of the phase of the impedance as a function of logarithm of the pulsation is presented in Fig. 9 and 10.

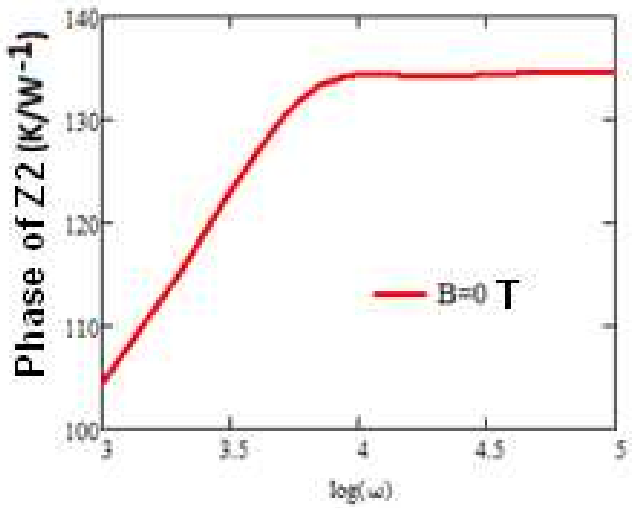

Fig. 9: Phase of the thermal impedance according to the logarithm of the pulsation without magnetic field (D=26cm2/scm/s H=0.03µm, a=1cm2/s, k=1,54 W/cm °C)

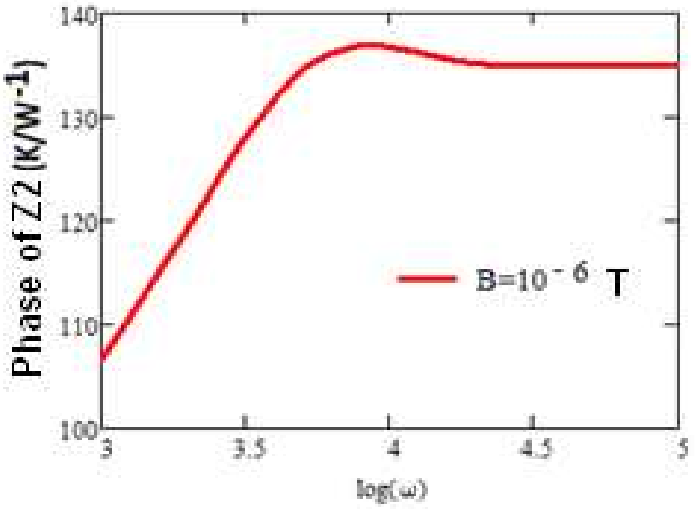

Fig. 10: Phase of the thermal impedance according to the logarithm of the pulsation in the presence of a magnetic field (D=26 cm^2/s H=0.03 µm, a=1cm^2/s, k=1, 54 W/cm. °C)

The phase of the impedance increases for the pulsations ranging between 10^3rad/s and 10^4rad/s then decreases lightly before remaining constant for the higher frequencies. The application of the magnetic field increases the amplitude of the phase.

Nyquist Representation of the Impedance for an Illumination by the Back Face

Nyquist representation, Fig. 11 and 12, shows the evolution of the imaginary part of impedance as a function of its real part.

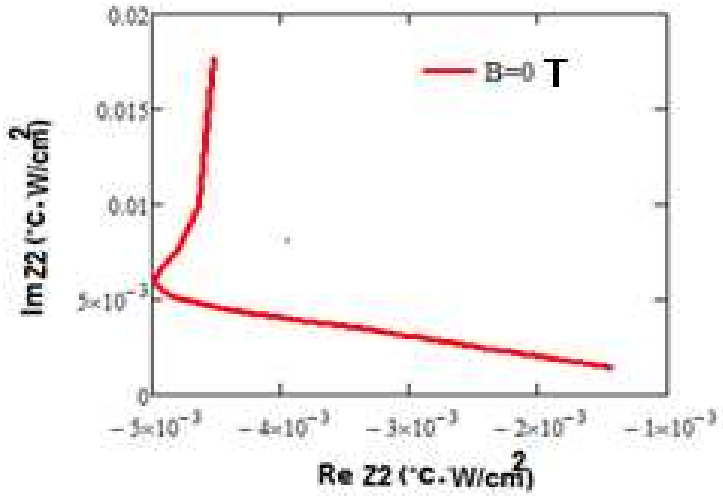

Figure 11: Imaginary part according to the real part of the impedance without magnetic field

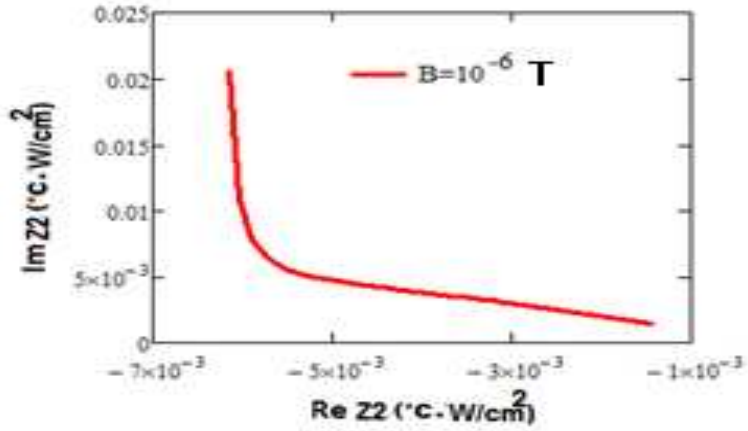

Figure 12: Imaginary part according to the real part of the impedance in the presence of a magnetic field

The diagram of Nyquist of the thermal impedance puts forwards the predominance of the capacitive phenomena.

Equivalent Electric Circuit of the Impedance

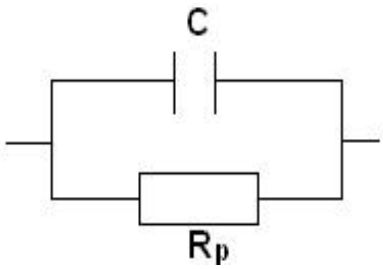

Fig. 12: Equivalent circuit of the thermal impedance without magnetic field applied

The diagram of figure 12 represents the equivalent electrical circuit which characterizes the effects observed starting from the diagrams of Bode (fig. 7, 8 and 9). C is the capacity and R_P parallel resistance.

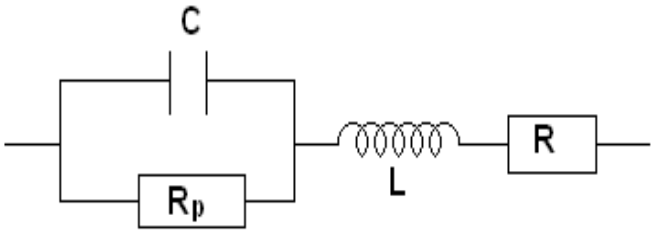

Fig. 13: Equivalent circuit of the thermal impedance with magnetic field applied

The electrical circuit represented describes the two phenomena capacitive and inductive of the impedance (figure10, 11, 12 and 13) where C is the capacity and R_P parallel resistance.

Conclusion

The resolution of the continuity equation of the excess minority carriers in the base of the photo voltaic cell, allowed the study of certain phenomenological and electric parameters according to the frequency of modulation and the effect of the magnetic field.

The theoretical study of the photovoltaic cell lit by its face postpones enabled us to determine the density of the excess minority carriers, the temperature variation, the variation of the density flux of heat. We studied the influence of the pulsation and the magnetic field on these parameters. From the diagrams of Bode and Nyquist of the thermal impedance, we proposed models of equivalent electric diagrams.

A degradation of the intrinsic properties of the photovoltaic cell, through these various parameters, was noted. It is noticed that for illumination by the back face, the modules of the studied parameters are very weak in front of those of the parameters obtained for an illumination by the front face.

Nomenclature

B (Tesla) Intensity of the magnetic field

ω (rad.s^{-1}) Angular frequency

D_n^* (cm^2.s-1) Coefficient of diffusion of the minority carriers in the base

D*($cm^2.s^{-1}$) Complex coefficient of diffusion

δ(cm^{-3}) Density of the photo minority carriers created in the base according to depth x and of time t

G(x,t) ($cm^{-3}.s^{-1}$) Rate of generation according to depth x and time t

gε(x) ($cm^{-3}.s^{-1}$) Rate of generation according to depth x

H(µm) Thickness of the base

L_n^* (cm) Diffusion length of the minority carriers in the base

L_ω^*(cm) Complex diffusion length of the minority carriers in the base according to the frequency ω and of the magnetic field

K(λ) Constant in the expression of the density of the carriers

λ_g The wavelength of cut of the semiconductor estimated at 1,12 µm

λ_0 The minimal wavelength of the source of light is equal to 0,3 µm

α(λ) (cm-1) Absorption coefficient to the wavelength λ

R(λ) Coefficient of reflection of material to the wavelength λ

To (°C) initial temperature of the photo voltaic cell

ΔT(°C) Temperature variation

Z(°C/W) Thermal impedance

Φ(λ) (cm-2/s) Incidental flow

k(W/cm/°C) Thermal conductivity

Φ(W/cm2) is the density flux of heat

Eg (ev) Energy of gap of silicon

$\sigma(\omega)$ Thermal coefficient of diffusion process

ρ (g/dm3) Density of volume of silicon

C(J/g/°C) Specific heat of silicon

References

[1] F.I. Barro, E. Nanema, A. Wereme, F. Zougmore and G. Sissoko, Recombination parameters measurement in silicon double sided surface field solar cell, *J. Des. Sci.*, 1(1) (2001), 76-80.

[2] R.M.L.Q. Nam, J. Nijs, M. Ghannam and J. Coppye, Spectral response of solar cells of high efficiency multi crystalline silicon, *J. Phys. III*, 2(7) (1992), 1305-1316.

[3] O.H. Lemra-bott, I. Ly, A.S. Maiga, A. Wereme, F.I. Barro and G. Sissoko, Bulkand surface recombination parameters measurement in silicon double sided solar cell under constant monochromatic illumination, *J. Sci.*, 8(1) (2008), 44-50.

[4] J.N. Hollenhorst and G. Hasnain, Frequency dependent hole diffusion in InGaAs double hetero structures, *Appl.Phys.Lett.*, 67(15) (1995), 2203-2205.

[5] A. Neugroschel, P.J. Chen, S.C. Pao and F.A. Lindholm, Experimental determination of series resistance of p-n junction diodes and solar cells, *IEEE Transactions on Electron Devices*, 25(March) (1978), 386-388.

[6] A. Dieng, O.H. Lemrabott, A.S. Maiga, A. Diao and G. Sissoko, Impedance spectroscopy method applied to electrical parameters determination on bifacial silicon solar cell under magnetic field, *J. of Sci.*, 7(3) (2007), 48-52.

[7] H.L. Diallo, A. Wereme, A.S. Maiga and G. Sissoko, New approach of both junction and back surface recombination velocities in a 3D modelling study of a polycrystalline silicon solar cell, *Eur. Phys. J. Appl. Phys.*, 42(2008), 203-211.

[8] M.M. Dème, S. Sarr, R. Sam, S. Gueye, M.L. Samb, F.I. Barro and G. Sissoko, Influence of grain size, the recombination velocity at grain boundaries and the angle of incidence of light on the enlargement of the space charge zone of a solar cell monofaciale, *J. Sci.*, 9(2) (2009), 17-27.

[9] M.S.O. Brahim, I. Diagne, S. Tamba, F. Niang and G. Sissoko, Characterization of the minimum effective layer of thermal insulation material two plaster from the method of thermal impedance, *Res. J. Appl. Sci. Eng. Techn.*, 3(4) (2011), 338-344.

[10] I. Ly, I. Zerbo, M. Wade, M. Ndiaye, A. Dieng, A. Diao, N. Thiam, A. Thiam, M.M. Dione, F.I. Barro, A.S. Maiga and G. Sissoko, Bifacial silicon solar cell under frequency modulation and monochromatic illumination: Recombination velocities and associated equivalent electrical circuits, *Proceedings of the 26th European Photovoltaic Solar Energy Conference and Exhibition*, (2011), Hamburg, Germany.

[11] A. Mandelis, Coupled ac photocurrent and photothermal reflectance response theory of semiconducting p-n junctions, *Journal of Applied Physics*, 66(11) (December) (1989), 5572-5583.

[12] I. Diagne, B. Fleur, M.O. Sidya, S. Gaye and G. Sissoko, Determination of the thermal parameters of a material in frequential dynamic mode starting from diagrams of Bode and representations of Niquist, *J. Sci.*, 8(2) (2008), 88-98.

[14] N. Thiam, A. Diao, M. Wade, M. Ndiaye, I. Zerbo, M. Sarr, A.S. Maïga and G. Sissoko, Study of the photothermal response of a monofacial solar cell in dynamic regime under a multispectral illumination, *Research Journal of Applied Sciences, Engineering and Technology*, 5(1) (2013), 134-141.

[15] M.F. Mbaye, M. Zoungrana, N. Thiam, A. Diao, G. Sahin, M. Ndiaye, M. Dieng and G. Sissoko, Study of the photo thermal response of a mono facial solar cell in dynamic regime under a multispectral illumination and under magnetic field, *International Journal of Inventive Engineering and Sciences (IJIES)*, 1(11) (2013), 60-66.